J. Electrochem. Sci. Eng. **14(6)** (2024) 835-843; http://dx.doi.org/10.5599/jese.2519

Open Access : : ISSN 1847-9286
www.jESE-online.org

Original scientific paper

Alkaline etching of diffusion zinc coatings NiZn and CoZn as promising electrocatalysts for hydrogen evolution reaction

Natalya Amelina✉, Daria Zakharova, Alexander Biryukov✉, Dmitry Zakharyevich and Maxim Ulyanov

Chelyabinsk State University, 454001 Chelyabinsk, Russian Federation

Corresponding authors: ✉ amelina-natasha@mail.ru; ✉ st4857@yandex.ru; *Tel.: +7(351)799-70-69*

Received: October 3, 2024; Accepted: October 28, 2024; Published: November 18, 2024

Abstract

Coatings based on NiZn and CoZn alloys were obtained by combining electrodeposition and diffusion galvanizing methods. The coatings are homogeneous and uniform, the zinc concentration is between 85.0 to 89.5 at.%, and consist of intermetallic phases of NiZn and CoZn, mainly γ-Ni_2Zn_{11} and γ_2-$CoZn_{13}$. Alkaline etching of coatings is accompanied by selective dissolution of zinc, and the rate of dissolution of coatings increases with time. This dealloying is accompanied by a change in the morphology of the coatings - cracks, pits, and pores of considerable depth are formed. These defects contribute to the formation of galvanic coupling between the coating and the substrate, which leads to an increase in the dissolution rate. The electrochemical behavior of coatings after alkaline etching in the cathodic hydrogen evolution reaction was studied. The cathodic current of hydrogen evolution on coatings alkaline etching increases by 1.5 to 3 times compared to coatings before etching. This effect is greater on Ni-based coatings. Diffusion galvanizing followed by dealloying is a promising method for creating electrode materials for alkaline electrolysis with hydrogen evolution.

Keywords

Etched alloy coatings; dealloying; surface morphology; water electrolysis; cathodic polarization

Introduction

Hydrogen is a valuable chemical product and energy carrier. The main advantages of hydrogen as an energy source are its high energy intensity and low environmental impact. Hydrogen is produced industrially by methane conversion, coal gasification, alkaline electrolysis of water and other methods. The advantage of steam conversion and coal gasification is high productivity, but the use of these technologies is associated with a large amount of CO_2 emissions into the atmosphere. The advantages of electrolysis include relative simplicity, high purity of hydrogen, and

availability of raw materials. The important thing is that water electrolysis is a more environmentally friendly way to produce hydrogen and does not lead to the accumulation of CO_2 in the atmosphere.

Alkaline electrolysis on the electrodes is accompanied by hydrogen evolution reaction (HER) and oxygen evolution reaction (OER), which have a relatively low speed and require a high overpotential. To increase the efficiency of electrolysis, it is necessary to use electrodes with high catalytic activity, as well as corrosion resistance in alkaline solutions. The most effective electrocatalysts for both HER and OER are materials based on platinum group metals. Platinum has the lowest hydrogen evolution overvoltage and high corrosion resistance. However, noble metals are inaccessible and expensive, which makes their use often impractical. An alternative to platinum group metals in water electrolysis can be metals of the iron triad, especially nickel. Nickel and its compounds demonstrate high catalytic properties, and in addition, nickel is stable in an alkaline environment. Several major reviews have recently been published on the use of nickel and its compounds as electrocatalysts for hydrogen evolution reaction [1-3]. However, nickel-based electrodes need to be improved and increased in efficiency. The main strategies for improving nickel-based electrode materials are surface modification of nickel metal or its alloys; synthesis of nickel oxides, hydroxides, sulfides and phosphides using an electrically conductive carbon matrix; use of nickel alloys [4-13]. Currently, electrodes are produced by electrodeposition of nickel, but the issue of increasing surface activity still remains open [14-18].

Here, we propose to use dealloying, which has previously proven itself well in the manufacture of nanoporous metals from precursor alloys containing aluminum or zinc as an electronegative component, to increase the surface area and catalytic activity of nickel-based coatings [19,20]. MeZn coatings can be obtained by combining electrochemical deposition of Ni, Co or their alloy CoNi on steel substrate and subsequent diffusion galvanizing in zinc powders with a nanostructured particle surface to obtain NiZn, CoZn and CoNiZn coatings [21-24].

The purpose of the work is to study the alkaline etching of diffusion coatings based on nickel, cobalt and zinc and the electrochemical activity of the dealloyed coatings in the hydrogen evolution reaction.

Experimental

Materials

The coatings were applied to substrates made of structural alloyed chromium steel. Before applying coatings, disc-shaped substrates were ground with sandpaper with a successive decrease in grain size from P1000 to P2500 and degreased in a solution (g/l): 10 $NaHCO_3$, 5 NaOH; 0.01 anionic surfactant at a temperature of 50±1 °C for 10 minutes. After degreasing, the substrates were washed in hot and cold distilled water. Before coating, the substrates were activated in a 10 wt.% H_2SO_4 solution for 10-15 seconds at a temperature of 25±1 °C and then washed in distilled water.

For electrodeposition of NiCo coatings, the following electrolyte was used [25] (g/l): 25 H_3BO_3, 35 $CoSO_4{\cdot}7H_2O$; 246 $NiSO_4{\cdot}7H_2O$, (pH~4.4). For electrodeposition of Co coatings, $NiSO_4{\cdot}7H_2O$ was excluded from the electrolyte, and for electrodeposition of Ni coatings, $CoSO_4{\cdot}7H_2O$ was excluded from the electrolyte. All coatings were applied at a cathodic current density of 20 $mA{\cdot}cm^{-2}$ for 60 minutes at a temperature of 25±1 °C. Galvanic coatings were subjected to diffusion galvanizing in zinc powders with a nanostructured particle surface according to the method described in the works [26,27]. Diffusion galvanizing was carried out for 2 hours at a temperature of 450 °C. The thickness of the coatings was determined by the difference in mass before and after treatment.

Physical research methods

The chemical composition of the coatings was determined using an energy-dispersive X-ray fluorescence spectrometer ARL QUANT'X. The surface morphology of the samples was investigated using a scanning electron microscope JEOL JSM-6490 equipped with an energy dispersive spectrometer INCA DRY COOL for elemental analysis.

Determination of etch rate using gravimetry

The coatings were degreased with isopropyl alcohol and weighed with an accuracy of 0.0001 g. Etching was carried out in a solution of sodium hydroxide NaOH (reagent grade) 5 mol/l. The samples were periodically removed from the alkali solution, washed with distilled water, dried with filter paper, weighed on an analytical balance, and the weight loss was recorded, from which the fraction of the etched coating was calculated. The etching was repeated until active dissolution ceased.

Cathodic polarization curves

To study the reaction of hydrogen evolution, cathodic polarization curves of the coatings were obtained in a solution of NaOH (reagent grade) 0.1 mol/l. A silver/silver chloride electrode (4.2 mol/l KCl) was used as a reference electrode, and graphite was used as an auxiliary electrode. The cathodic polarization was 1.0 V from the open circuit potential, the potential sweep rate was 0.02 V s^{-1}.

Results and discussion

Physico-chemical characteristics of coatings

Uniform homogeneous coatings based on Ni, Co and NiCo alloys were obtained by electrodeposition (hereinafter, the coatings are indicated by symbols of chemical elements). Table 1 presents the average thicknesses *l* and current outputs for the coatings under study.

Table 1. *Characteristics of electrodeposited coatings*

Coating	*l* / µm	Current efficiency, %
Co	11±2	52±13
CoNi	14±1	70±4
Ni	15±2	72±6

The thickness of the coatings is in the range of 10 to 15 µm, while the current efficiency during the deposition of cobalt coatings decreases by 20 % compared to the deposition of Ni and CoNi coatings. This can be explained by differences in the concentrations of nickel and cobalt salts in the original electrolyte. The concentration of $CoSO_4$ in the electrolyte is 7 times less than the concentration of $NiSO_4$ since, according to literature data, coprecipitation of nickel and cobalt proceeds according to an anomalous mechanism [28], that is, a metal with a more negative electrode potential $E^0(Co^{2+}/Co)$ = -0.277 V is deposited first, despite the presence in the solution of metal with a more positive electrode potential $E^0(Ni^{2+}/Ni)$ = - 0.250 V [28]. The chemical composition of the CoNi coating, according to the results of X-ray fluorescence spectroscopy, is Fe 16 ± 3 at.%; Co 43 ± 3 at.% and Ni 41 ± 4 at.%. The presence of iron can be explained by the relatively small thickness of the coatings (15 µm) and the influence on the analysis results of the steel substrate. However, it is clear that the Co:Ni ratio in the coating is 1:1. Electroplated Co, CoNi and Ni were subjected to diffusion galvanizing. The thickness and chemical composition of diffusion zinc coatings are given in Table 2.

The thickness of the coatings is in the range of 35-40 µm, and the Co:Zn ratio in CoZn coatings corresponds to the γ_2-phase $CoZn_{13}$, according to the Co-Zn phase diagram [29]. ForNiZn coatings, the

Zn concentration is 5 % lower, and the Ni:Zn ratio indicates the presence of the Ni_2Zn_{11} γ-phase in the coatings [30]. The X-ray diffraction patterns of the obtained coatings confirm these conclusions (Figure 1). For the CoNiZn coatings with a zinc concentration of 89.0 at. %, the X-ray diffraction pattern contains a set of reflections from $CoZn_{13}$, Ni_2Zn_{11} and Co_2Zn_{11}, so the coating is heterophase.

Table 2. *Thickness and chemical composition of diffusion zinc coatings*

Coating	*l* / μm	Content, at.%		
		Co	Ni	Zn
CoZn	40±9	10.0±0.5	—	89.8±0.2
CoNiZn	36±4	6.0±1.0	5.0±1.0	89.0±0.3
NiZn	39±10	—	15.0±1.0	85.1±0.3

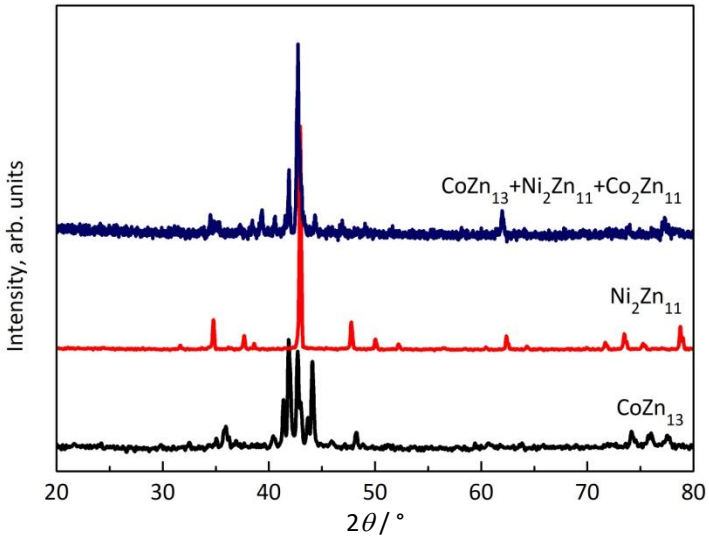

Figure 1. *X-ray diffraction patterns of coatings: CoZn (bottom, blue), NiZn (middle, red) and CoNiZn (top, black). The phases identified in the diffraction patterns are indicated. The Co_2Zn_{11} phase is isostructural with the Ni_2Zn_{11} phase but with a larger lattice parameter*

Etching of coatings

CoZn, NiZn and CoNiZn coatings were etched in NaOH solution to obtain a morphologically developed and catalytically active surface. Figure 2 shows the dependence of the fraction of etched coating on the etching time.

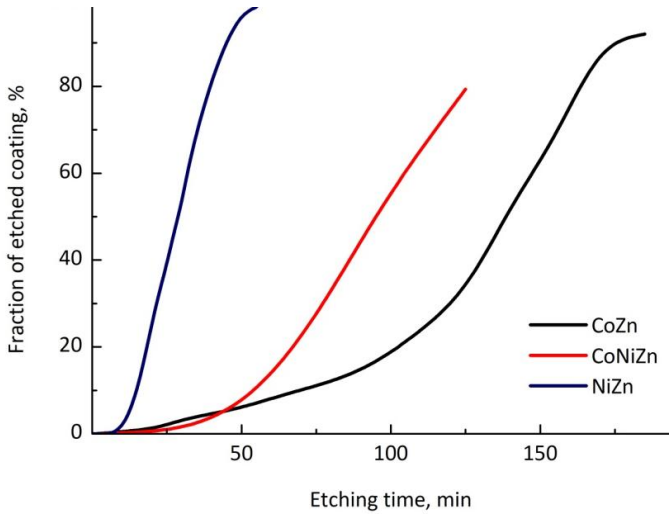

Figure 2. *Dependences of the fraction of etched coating on the etching time of CoZn, NiZn and CoNiZn coatings in 5 mol/l NaOH solution*

The fraction of the etched coating was calculated based on the difference in mass before and after etching. The calculations only took into account the dissolution of zinc during etching, assuming that other metals do not dissolve.

The dependences can distinguish the initial stage with a relatively low dissolution rate and a slow increase in speed, and the main stage at which the dissolution rate increases sharply. The duration of the initial stage depends on the chemical nature of the coatings. Thus, the duration of the initial stage for NiZn coatings is 10 times shorter than for CoZn coatings. Half of the NiZn coating is etched off in 20 minutes, CoNiZn coating in 80 minutes, and CoZn coating in 120-130 minutes. NiZn coatings dissolve at a faster rate than other coatings.

Figure 3 shows SEM images of coatings after etching in 5 mol/l NaOH solution. On the surface of all coatings, there are many cracks ranging in width from one to tens of micrometers. CoZn coatings have crack widths of more than 10 µm and, under the etched coating layer, another layer is visible, also covered with cracks, but of a smaller size. The width of cracks in the CoNiZn coating reaches 10 µm. NiZn coatings have more cracks with sizes up to 10 µm. On all coatings, cracks intersect and divide the surface into sections. Each section, in turn, is also covered with cracks of different sizes. On NiZn coatings, irregularly shaped pores can be seen; cracks create a grainy pattern.

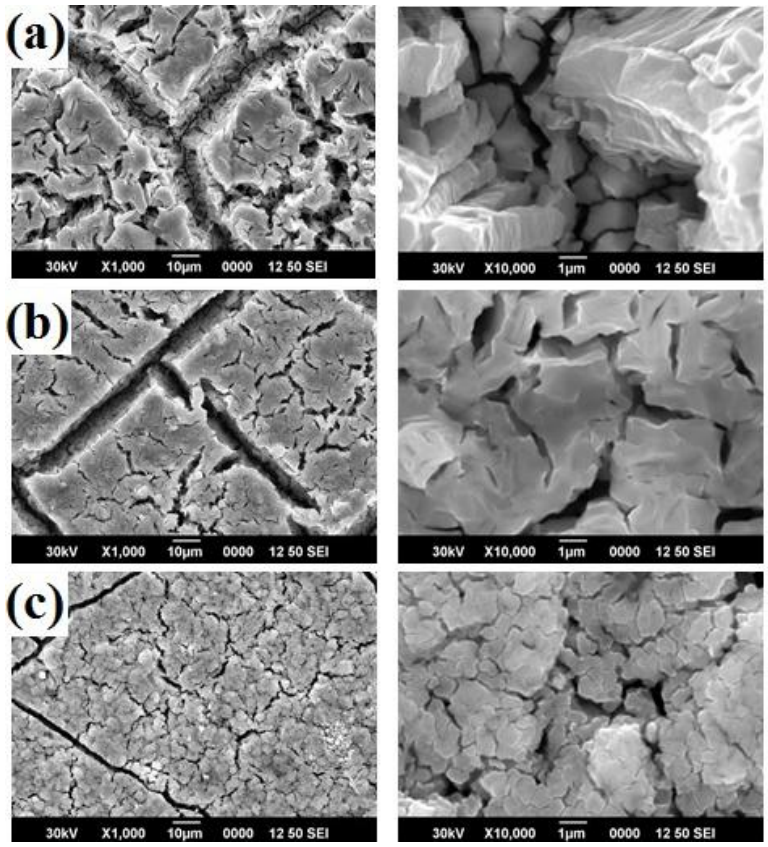

Figure 3. *SEM images of coatings after etching in 5 mol/l NaOH solution: (a) CoZn, (b) CoNiZn, (c) NiZn*

Table 3 presents the results of determining the chemical composition of the coating surface after etching.

Table 3. *Chemical composition of coatings after etching in 5 mol/l NaOH solution*

Coating	Content, at.%				
	O	Fe	Co	Ni	Zn
CoZn	8.8	0.9	64.4	—	25.9
CoNiZn	9.5	0.8	29.1	28.4	32.2
NiZn	16.9	1.1	—	53.8	28.2

The Zn concentration decreased from 25 to 32 at.%, but a complete zinc etching did not occur. The concentrations of cobalt and nickel increased significantly compared to unetched coatings (4 times for NiZn and 6.5 times for CoZn, respectively). The concentrations of Ni and Co in the CoNiZn coating also increased, and the Ni:Co ratio of 1:1 was maintained. A small amount of iron in the analysis results may be due to the influence of the steel substrate on the analysis result, especially if there are deep cracks in the coatings. Some oxygen appears on the surface due to oxidation during etching.

Thus, the etching of coatings is accompanied by the preferential dissolution of zinc from the intermetallic phases NiZn and CoZn. It is known that with the dealloying in surface layers, the concentration of electropositive metal increases, and, in addition, the morphological development of the surface occurs due to the formation of cracks and pores. The first section in the kinetic etching curves of coatings is apparently associated with selective dissolution and the appearance of cracks. The accumulation of an electropositive element and the morphological development of the surface leads to the appearance of galvanic coupling, both between areas of the coating with different concentrations of Ni or Co, and between the coating and the substrate. Deep cracks can act as channels through which a corrosive environment reaches the substrate. In this way, a three-dimensional coating dissolution front is formed. Galvanic coupling enhances the corrosion of the coating and increases the rate of dissolution, which is characterized by the appearance of a second section on the kinetic curves. The result is a developed, active surface with a relatively high concentration of active nickel or cobalt, which can accelerate the hydrogen evolution reaction.

Cathodic polarization curves

Figures 4 to 6 show the cathodic polarization curves of the materials under investigation. The cathodic curves of galvanic coatings of Co, NiCo and Ni, which were subjected to diffusion zinc plating followed by etching (indicated on the graphs by the etching fraction in %), were compared with the cathodic curves of galvanic coatings that were not subjected to treatment (indicated on the graphs by the symbols of the corresponding chemical elements). It can be seen that with increasing etching fraction, the cathodic current density increases, which apparently indicates an increase in the intensity of hydrogen evolution. Compared to coatings that were not treated, an increase in cathodic current occurs only with an etching fraction above 10 %. For CoZn coatings, an increase in etching up to 90 % leads to a 2-fold increase in cathodic current compared to an untreated Co coating. For CoNiZn coatings, the current increases by 1.6 times, and for NiZn coatings by 3 times. Thus, the maximum cathodic current is observed in NiZn coatings after etching.

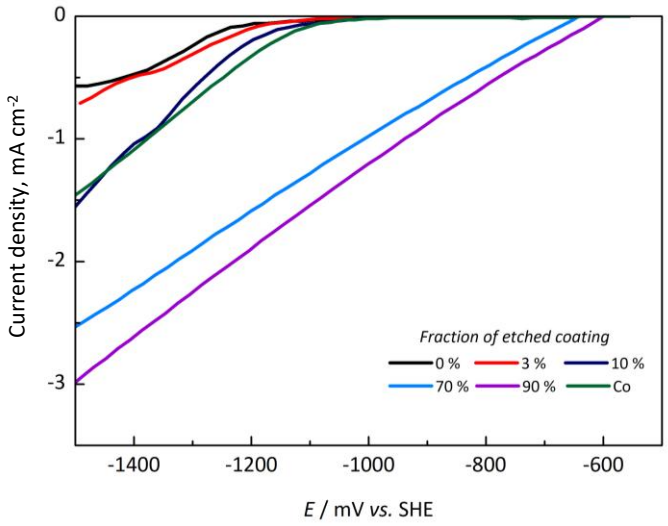

Figure 4. *Cathodic polarization curves of CoZn after etching in 5 mol/l NaOH solution*

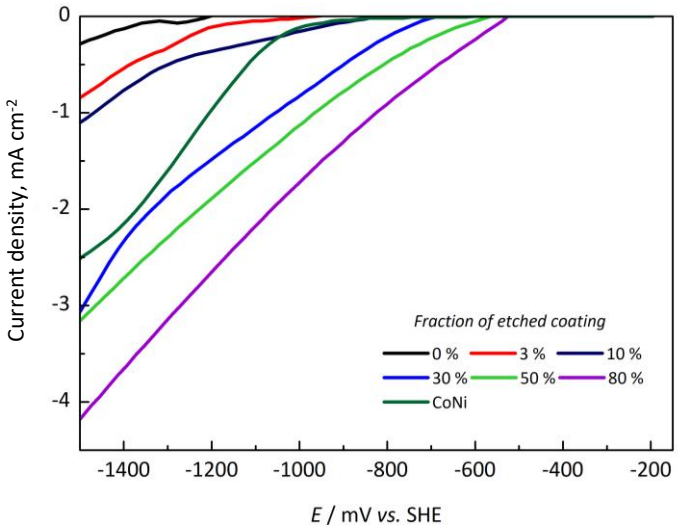

Figure 5. *Cathodic polarization curves of CoNiZn after etching in 5 mol/l NaOH solution*

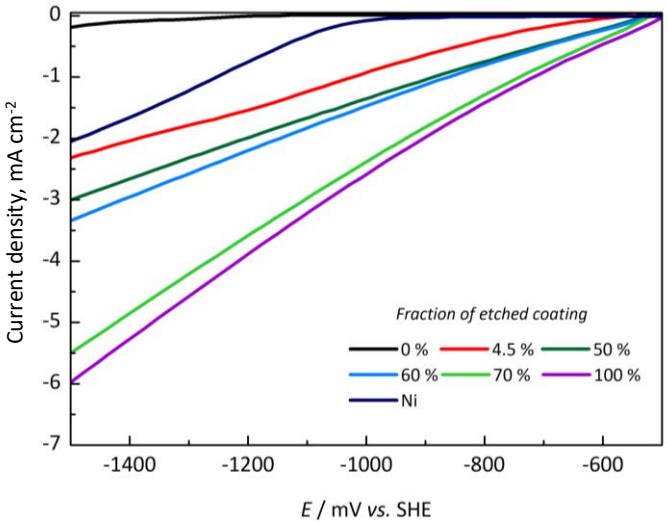

Figure 6. *Cathodic polarization curves of NiZn after etching in 5 mol/l NaOH solution*

Conclusions

As a result of diffusion galvanizing of Co, CoNi and Ni galvanic coatings, CoZn, CoNiZn and NiZn coatings with a zinc concentration of 85.0 to 89.5 % were obtained. When etching in an alkaline solution, the morphological development of the coating surface occurs, accompanied by an increase in the corrosion rate, apparently due to the formation of galvanic coupling between the coating areas and the substrate. Treatment of coatings leads to an increase in the cathodic current of the hydrogen evolution reaction by 1.5 to 3 times. The cathodic current increases as the etching fraction increases. NiZn coatings have the maximum cathodic current. The combination of alloying galvanic coatings with zinc and alkaline etching makes it possible to obtain materials that are promising for use in the alkaline electrolysis of water.

References

[1] N. A. Khan, G. Rahman, T. M. Nguyen, A. U. I. H. A. Shah, C. Q. Pham, M. X. Tran, D. L. T. Nguyen, Recent Development of Nanostructured Nickel Metal-Based Electrocatalysts for Hydrogen Evolution Reaction, *Topics in Catalysis* **66(1)** (2023) 149-181. https://doi.org/10.1007/s11244-022-01706-2

[2] F. Zhou, Y. Zhou, G. G. Liu, C. T. Wang, J. Wang, Recent advances in nanostructured electrocatalysts for hydrogen evolution reaction, *Rare Metals* **40** (2021) 3375-3405. https://doi.org/10.1007/s12598-021-01735-y
[3] N. Lotfi, G.B. Darband, A review on electrodeposited metallic Ni-based alloy nanostructure for electrochemical hydrogen evolution reaction, *International Journal of Hydrogen Energy* **70** (2024) 301-314. https://doi.org/10.1016/j.ijhydene.2024.05.121
[4] Y. W. Phuan, E. Ibrahim, M. N. Chong, T. Zhu, B. K. Lee, J. D. Ocon, E. S. Chan, *In situ* Ni-doping during cathodic electrodeposition of hematite for excellent photoelectrochemical performance of nanostructured nickel oxide-hematite p-n junction photoanode, *Applied Surface Science* **392** (2017) 144-152. https://doi.org/10.1016/j.apsusc.2016.09.046
[5] Z. Xing, L. Gan, Experimental and theoretical insights into sustained water splitting with an electrodeposited nanoporous nickel hydroxide@nickel film as an electrocatalyst, *Journal of Materials Chemistry A* **5(17)** (2017) 7744-7748. https://doi.org/10.1039/D4TA03872J
[6] H. Han, S. Park, D. Jang, W. B. Kim, N-doped carbon nanoweb-supported Ni/NiO heterostructure as hybrid catalysts for hydrogen evolution reaction in an alkaline phase, *Journal of Alloys and Compounds* **853** (2021) 157338. https://doi.org/10.1016/j.jallcom.2020.157338
[7] C. Song, X. Zhou, S. J. Yoo, Z. Zhang, X. Zhang, J. G. Kim, W. Zhang, Highly electrochemically-active surface area of $Ni(OH)_2$ with petal structure in situ grown on conductive Ni foam for efficient hydrogen evolution reaction, *Surface and Interface Analysis* **53(12)** (2021) 1020-1026. https://doi.org/10.1002/sia.7002
[8] J. Hu, S. Li, Y. Li, J. Wang, Y. Du, Z. Li, X. Han, J. Sun, P. Xu, A crystalline-amorphous Ni-$Ni(OH)_2$ core-shell catalyst for the alkaline hydrogen evolution reaction, *Journal of Materials Chemistry A* **8(44)** (2020) 23323-23329. https://doi.org/10.1039/D0TA08735A
[9] Z. Yao, J. Wang, Y. Wang, T. Xie, C. Li, Z. Jiang, Boosting electrocatalytic activity toward alkaline hydrogen evolution by strongly coupled ternary Ni_3S_4/Ni/$Ni(OH)_2$ hybrid, *Electrochimica Acta* **382** (2021) 138342. https://doi.org/10.1016/j.electacta.2021.138342
[10] F. Ganci, B. Patella, E. Cannata, V. Cusumano, G. Aiello, C. Sunseri, P.Mandin, R. Inguanta, Ni alloy nanowires as high efficiency electrode materials for alkaline electrolysers, *International Journal of Hydrogen Energy* **46(72)** (2021) 35777-35789. https://doi.org/10.1016/j.ijhydene.2020.11.208
[11] B. Buccheri, F. Ganci, B. Patella, G. Aiello, P. Mandin, R. Inguanta, Ni-Fe alloy nanostructured electrodes for water splitting in alkaline electrolyser, *Electrochimica Acta* **388** (2021) 138588. https://doi.org/10.1016/j.electacta.2021.138588
[12] X. Zetao, D. Quintero, S. Kitano, T. Nagao, M. Iwai, Y. Aoki, K. Fushimi, H. Habazaki, Preparation of highly active and durable electrodes for alkaline water electrolysis by anodizing of commercial FeNi and FeNiCo alloys, *Electrochimica Acta* **491** (2024) 144352. https://doi.org/10.1016/j.electacta.2024.144352
[13] S. Carbone, F. Proietto, F. Bonafede, R.L. Oliveri, B. Patella, F. Ganci, G. Aiello, P. Mandin, M. Kim, M. Scopelliti, R. Inguanta, Behavior of a forest of NiFe nanowires in KOH and NaCl solution for water electrolysis, *Electrochimica Acta* **467** (2023) 143120. https://doi.org/10.1016/j.electacta.2023.143120
[14] F. Ganci, B. Buccheri, B. Patela, E. Cannata, G. Aiello, P. Mandin, R. Inguanta, Electrodeposited nickel-zinc alloy nanostructured electrodes for alkaline electrolyzer, *International Journal of Hydrogen Energy* **47(21)** (2022) 11302-11315. https://doi.org/10.1016/j.ijhydene.2021.09.221
[15] D.V. Burlyaev, O.A. Kozaderov, P. Volovitch, Zinc-nickel alloy coatings: kinetics of electrodeposition, corrosion and selective dissolution, *Condensed Matter and Interphases* **23(1)** (2021) 3-15. https://doi.org/10.17308/kcmf.2021.23/3292
[16] Y. Sako, R. Saeki, M. Hayashid, T. Ohgai, Uniaxial Magnetization and Electrocatalytic Performance for Hydrogen Evolution on Electrodeposited Ni Nanowire Array Electrodes with Ultra-High Aspect Ratio, *Nanomaterials* **14(9)** (2024) 755. https://doi.org/10.3390/nano14090755

[17] C. Li, H. Pang, R. Xu, J. Fan, E. Liu, T. Sun, CoFe-Layered Double Hydroxide Needles on MoS_2/Ni_3S_2 Nanoarrays for Applications as Catalysts for Hydrogen Evolution and Oxidation of Organic Chemicals, *ACS Applied Nano Materials* **7(6)** (2024) 6449-6459. https://doi.org/10.1021/acsanm.4c00186
[18] F. Ganci,V. Cusumano, P. Livreri, G. Aiello, C. Sunseri, R. Inguanta, Nanostructured Ni-Co alloy electrodes for both hydrogen and oxygen evolution reaction in alkaline electrolyzer, *International Journal of Hydrogen Energy* **46(16)** (2021) 10082-10092. https://doi.org/10.1016/j.ijhydene.2020.09.048
[19] Q. Zhou, C. Xu Y. Li, X. Xie, H. Liu, S. Yan, Synergistic coupling of NiFeZn-OH nanosheet network arrays on a hierarchical porous NiZn/Ni heterostructure for highly efficient water splitting, *Science China Materials* **65(5)** (2022) 1207-1216. https://doi.org/10.1007/s40843-021-1926-9
[20] N. Lotfi, M. Aliofkhazraei, H. Rahmani, G. B. Darband, Zinc-nickel alloy electrodeposition: characterization, properties, multilayers and composites, *Protection of Metals and Physical Chemistry of Surfaces* **54** (2018) 1102-1140. https://doi.org/10.1134/S2070205118060187
[21] P. De Lima-Neto, A. N. Correia, R. P. Colares, W. S. Araujo, Corrosion Study of Electrodeposited Zn and Zn-Co Coatings in Chloride Medium, *Journal of the Brazilian Chemical Society* **18(6)** (2007) 1164-1175. https://doi.org/10.1590/S0103-50532007000600010
[22] M. Tomić, M. M. Petrović, S. Stanković, S. I. Stevanović, J. B. Bajat, Ternary Zn-Ni-Co alloy: Anomalous codeposition and corrosion stability, *Journal of the Serbian Chemical Society* **80(1)** (2015) 73-86. https://doi.org/10.2298/JSC260814113B
[23] R. S. Bhat, V. B. Shet, Development and characterization of Zn-Ni, Zn-Co and Zn-Ni-Cocoating, *Surface Engineering* **36(4)** (2020) 429-437. https://doi.org/10.1080/02670844.2019.1680037
[24] Yu. I. Marygina, S. A. Kaluzhina, I. V. Protasova, Phase Composition and Morphology of Ni, Zn-alloy Surface, Electrodeposited from Sulfate-ammonium Solution, *Condensed Matter and Interphases* **20(1)** (2018) 93-101. https://doi.org/10.17308/kcmf.2018.20/481
[25] A. M. Abd El-Halim, On the anomalous phenomenon of Co-Ni alloy electrodeposition, *Surface Technology* **23(3)** (1984) 207-213. https://doi.org/10.1016/0376-4583(84)90013-X
[26] A. I. Biryukov, D. A. Zakharyevich, R. G. Galin, N. Devyaterikova, I. Scherbakov, Corrosion resistance of thermal diffusion zinc coatings of PNTZ in oilfield environments, *EDP Sciences* **121** (2019) 02005. https://doi.org/10.1051/e3sconf/201912102005
[27] R. G. Galin, N. A. Shaburova, D. A. Zakharyevich, Thermal Diffusion Galvanizing in Ferriferous Zinc Powder, *Materials Science Forum* **870** (2016) 129-134. https://doi.org/10.4028/www.scientific.net/MSF.870.129
[28] A. Chitharanjan Hegde, V. Thangaraj, Electrodeposition and characterization Zn-Co Alloy, *Russian Journal of Electrochemistry* **45(7)** (2009) 756-761. https://doi.org/10.1134/S1023193509070076
[29] H. Okamoto, Co-Zn (Cobalt-Zinc), *Journal of Phase Equilibria and Diffusion* **28(3)** (2007) 315. https://doi.org/10.1007/s11669-007-9050-9
[30] G. P. Vassilev, T. Gomez-Acebo, J.-C. Tedenac, Thermodynamic optimization of the Ni-Zn system, *Journal of Phase Equilibria* **21** (2000) 287-301. https://doi.org/10.1361/105497100770340075